Computers and Chemical Engineering 150 (2021) 107327

Contents lists available at ScienceDirect

Computers and Chemical Engineering

journal homepage: www.elsevier.com/locate/compchemeng

A generic superstructure modeling and optimization framework on the example of bi-criteria Power-to-Methanol process design

Philipp Kenkel[a,b,*], Timo Wassermann[a,b], Celina Rose[a], Edwin Zondervan[c]

[a] University of Bremen, Advanced Energy Systems Institute, Enrique-Schmidt Straße 7, 28359 Bremen, Germany
[b] University of Bremen, artec Sustainability Research Center, Enrique-Schmidt Straße 7, 28359 Bremen, Germany
[c] Department of Chemical Engineering, Twente University, 7522NB Enschede, Netherlands

ARTICLE INFO

Article history:
Received 15 December 2020
Revised 5 March 2021
Accepted 10 April 2021
Available online 13 April 2021

Keywords:
Power-to-Methanol
Superstructure optimization
Heat integration
Python
Open source

ABSTRACT

This work presents a fully open-source superstructure optimization model for bi-criteria process design optimization. This model is implemented in the ***O**pen s**U**perstruc**T**ure mo**D**eling and **O**ptimizati**O**n f**R**amework* (OUTDOOR). It combines mass, energy and cost balances with a more sophisticated heat integration concept with low computational effort and acceptable accuracy. The model is applied to a Power-to-Methanol (PtM) process design case study. A cost optimal methanol plant is identified at net production costs (NPC) of 892 €/t_{MeOH} and net production emissions (NPE) of -1.937 $t_{CO2\text{-}eq.}/t_{MeOH}$. It utilizes CO_2 captured from refinery flue gas and hydrogen supply via. ambient pressure alkaline electrolysis. A plant configuration, designed for minimum CO_2 emissions yields costs of 979 €/t_{MeOH} with emissions of -2.191 $t_{CO2\text{-}eq.}/t_{MeOH}$, using CO_2 from ambient air and refinery and cement factory flue gases. A sensitivity analysis on electricity prices forecasts cost competitive methanol at large production capacities and low electricity prices of 2 ct/kWh.

1. Introduction

Superstructure optimization is a tool for process synthesis utilizing mathematical models and optimization algorithms to identify optimal process design for different production systems. A superstructure represents a large number of possible flowsheets. Every unit-operation inside this superstructure can be described by the same set of generic equations representing different processing tasks such as mixing, reaction, separation or utility consumption (Yeomans and Grossmann, 1999) (Bertran et al., 2017) . The unit-operations and flowsheet options are formulated as a mathematical model. Using this model an optimization solver identifies the best flowsheet for a given objective function (Quaglia et al., 2015; Zondervan et al., 2011).

Superstructure optimization can be used for various applications. For example, it was utilized for heat exchanger network optimization by Yee and Grossmann and Ciric and Floudas (Ciric and Floudas, 1991; Yee and Grossmann, 1990). Nowadays it is often applied in the design of biorefineries using different types of biomass, e.g. wheat straw or algae. Zondervan et al. proposed a superstructure optimization for a wheat straw biorefinery, while Gong et al. utilized superstructure optimization to identify cost-optimal algae biorefineries producing biodiesel and other value-added products (Gong and You, 2015; Zondervan et al., 2011). Meanwhile Galanopoulos et al. integrated a wheat straw and algae refinery for identification of synergies (Galanopoulos et al., 2019).

Superstructure optimization can also be applied to Power-to-X (PtX) processes where water and carbon dioxide are transformed into valuable products such as kerosene, methanol or methane by application of renewable electricity. Using this approach, Kenkel et al. identified cost and emission optimal methanol production from electrolysis and CO_2 capture, while Baliban et al. investigated process design of coal, biomass and natural gas to liquids via Fischer-Tropsch synthesis (Baliban et al., 2012; Kenkel et al., 2020).

It is apparent that superstructure models are very versatile, but they also bring a downside. These models can be formulated in different ways and are often very complex, being written as mixed-integer (non) linear programming models (MI(N)LP). Therefore, it has become common practice in science that every research group develops its own model and implements it for its specific case using commercial algebraic modeling software such as GAMS or

* Corresponding author.
E-mail address: kenkel@uni-bremen.de (P. Kenkel).

https://doi.org/10.1016/j.compchemeng.2021.107327
0098-1354/

Nomenclature

U	All processes / Unit-operations
U^{STOIC}	Stoichiometric reactors
U^{YIELD}	Yield reactors
U^{C}	Process units that are considered in CAPEX
U^{ELGEN}	Electricity generating units
$U^{HEATGEN}$	SH steam generating units
U^{PP}	Product pool
I	Chemical components
K	Fixed interval grid points for piece-wise linearisation
K^{I}	Fixed intervals for piece-wise linearisation
M	Reactants
R	Reactions
HI	Heat intervals
HI^{M}	Highest heat interval
HI^{LP}	Heat interval for LP steam
ACC_u	Annualized capital costs of unit-operation u
$CREDITS$	Emission credits as avoided burden
ACC_u	Annualized capital costs of unit-operation u
ACC_{hi}^{HEN}	Annualized capital costs of virtual heat exchanger on heat interval hi
ACC^{HP}	Annualized costs of heat pump
ACC_u^{RE}	Periodical recurring costs of unit-operation u
$CAPEX$	Total annualized capital costs
$C^{COOLING}$	Costs for total cooling demand
C^{EL}	Costs for total electricity demand
C^{HEAT}	Costs for total external heating demand
C^{M}	Yearly maintenance costs
C^{O}	Yearly operation costs
$C^{O\&M}$	Operating and Maintenance costs
C_u^{RM}	Costs for raw materials in unit-operation u
$C^{RM,TOT}$	Total raw material costs
C^{UT}	Costs for utilities
EC_u	Purchase equipment costs of unit-operation u
E_u^{EL}	Electricity demand of unit-operation u
$E^{EL,HP}$	Electricity demand of heat pump
$E_u^{EL,PROD}$	Electricity produced in unit-operation u
$F_{u',u,i}$	Flow from unit operation u' to u of component i
FCI_u	Fixed capital investment of unit operation u
$F_u^{ADD_1}$ / $F_u^{ADD_2}$	Externally added flow 1 and 2 to unit-operation u
$F_{u,i}^{ADD,TOT}$	Total externally added component i to unit-operation u
$F_{u,i}^{IN}$	Inlet flow of unit-operation u, component i
$F_{u,i}^{OUT}$	Outlet flow of unit-operation u, component i
$F_{u,i}^{WASTE}$	Waste flow of unit-operation u, component i
$F_i^{WASTE,TOT}$	Total waste flow of component i
$GWP^{CAPTURE}$	CO_2 emisions captured by capture technologies
GWP^{EL}	CO_2 emisions induced by external electricity supply
$GWP^{EMITTED}$	CO_2 emisions induced by unit operations
GWP^{HEAT}	CO_2 emisions induced by external heat supply
M_u^{CAPEX}	Reference flow for CAPEX calculation in unit-operation u
M_u^{EL}	Reference flow for electricity demand calculation of unit-operation u
M_u^{HEAT}	Reference flow for heat demand calculation of unit-operation u
$OPEX$	Total annual operational costs
$PROFITS$	Total annual profits
$Q_{u,hi}^{C}$	Cooling demand of unit-operation u on heat interval hi
Q^{COOL}	Total external cooling demand
Q_{hi}^{DEFI}	Heat deficit on heat interaval hi
Q_{hi}^{EX}	Exchanged heat on heat interval hi
$Q_{u,hi}^{H}$	Heat demand of unit-operation u on heat interval hi
Q^{HP}	Waste heat absorbed by heat pump
$Q^{HP,USE}$	Used heat from heat pump
Q_u^{PROD}	Produced super-heated steam by unit-operation u
$Q^{PROD,SELL}$	Produced super-heated steam that is sold to market
$Q^{PROD,USE}$	Produced super-heated steam that is used internally for heat supply
Q_{hi}^{RESI}	Residual heat on heat interval hi
$s_{u,k}^{CAPEX}$	S – Variale for SOS2 Constraint
TAC	Total annualized costs
Y_u	Binary decision variable of unit-operation u
Y_{hi}^{HEX}	Binary decision variable for heat exchanger on heat interval hi
$z_{u,k}^{CAPEX}$	Z – Variable for SOS2 Constraint
$\lambda_{k,u}$	Lambda-Variable for piece-wise linearization
b^{HEN}	Minimum CAPEX of virtual heat exchanger
$CECPI$	Chemical engineering plant index of the investigated year
$CECPI_u^{REF}$	Referance CECPI of a known unit-operation u
CON_u	Required concentration factor in unit-operation u
COP^{HP}	Coefficient of performance of heat pump
C_u^{REF}	Known reference costs of unit-operation u
c_u^{RE}	Percentage value of periodic costs in unit-operation u
EC^{HP}	Linear equipment costs of heatpump
f_u	Exponent for non-linear equipment cost calculation in unit-operation u
f_u^{ACC}	Annualization factor for unit-operation u
f_u^{DC}	Direct cost factor for unit-operation u
f_u^{IDC}	Indirect cost factor for unit-operation u
f_u^{M}	Maintenance cost factor for unit operation u
f^{O}	Operating cost factor
F^{PROD}	Desired yearly capacity of main product
$f(x)_{k,u}$	Pre-calcuted Equipment costs of unit-operation u in linear interval k
gwp_i	Global warming potential of component i
$gwp_u^{avoided}$	Global warming potential that can be avoided in productpool u
$gwp^{Electricity}$	Global warming potential of external electrictiy
gwp^{Heat}	Global warming potential of external steam
H	Full load operating hours per year
IR	Interest rate

LHV_i	Lower heating value of component i
LT_u	Lifetime in years of unit-operation u
$LT_u^{RE,y}$ / $LT_u^{RE,h}$	Periode of time (in years or hours) for periodic costs in unit-operation u
m^{HEN}	Slope for cost calculation of virtual heat exchanger
M_u^{REF} M^{REF}	Reference flow of a known unit-operation u equipment cost calculation
n^{PS}	Number of main process steps
n_u^{RE}	Number of periodic turnovers
T_{hi}	Grid temperature of heat interval hi
ΔT_u	Difference of inlet and outlet temperature in unit-operation u
ul_u^1 / ul_u^2	Upper limits for added flows 1 and 2 in unit-operation u
WH	Working personell hours per year
$x_{k,u}$	Pre-calcuated reference flows for non-linear EC calculation
α	Upper bound parameter for Big-M constraint
α^{HEX}	Upper bound paramter or Big-M constraint in HEX calculation
$\beta_{u,hi}^H$	Energy demand ration of unit-operation u in heat interval hi
$\gamma_{i,r,u}$	Stoichiometric reaction coefficion of component i, reaction r, unit u
δ_u^{PP}	Product price of product pool u
δ^{EL}	Electricity price
δ_{hi}^H	Steam price for heat interval hi
δ^{COOL}	Cooling water price
δ_i^{RM}	Raw material costs of component i
$\zeta_{u,i}$	Yield factor of unit-operation u and component i
η_u^{EL} / η_u^{HEAT}	Efficiency of electricity / heat generation in generator u
$\theta_{m,r,u}$	Stoichiometric conversion factor of reactant m, reaction r, unit u
$\kappa_{u,i}^{1,rhs}$ / $\kappa_{u,i}^{1,lhs}$	Binary parameter for component i in concentration calc. of unit u
$\kappa_{heat,\ u,i}^{1,\ ut}$	Binary paramter for component i in heat calc. of unit u
$\kappa_{el,\ u,i}^{1,\ ut}$	Binary paramter for component i in electricity calc. of unit u
$\kappa_{u,i}^{1,\ capex}$	Binary paramter for component i in equipment cost calc. of unit u
$\mu_{u,u',i}$	Splitfactor of unit-operation u, to unit-operation u', component i
$\rho_{u,i}^1/\rho_{u,i}^2$	Concentration of component i, in unit-operation u, added flow 1/2
$\tau_u^{HEAT,1}$ / $\tau_u^{HEAT,2}$	Specific heat demand 1 / 2 in unit-operation u
$\tau_u^{COOL,1}/\tau_u^{COOL,2}$	Specific cooling demand 1 / 2 in unit-operation u

AIMMS (Baliban et al., 2012; Bertran et al., 2017; Kong et al., 2016; Quaglia et al., 2015; Kravanja, 1990; Zondervan et al., 2011).

In recent work by Mencarelli et al. a review of different superstructure modeling approaches and existing software for superstructure construction and optimization is presented (Mencarelli et al., 2020). They point to Pro-CAFD as the most sophisticated tool featuring a graphical user interface and the ability to automatically generate process alternatives from sets of raw materials, products and reactions (Tula et al., 2017). Other software mentioned is P-Graph Studio, MIPSYN, SYNOPSIS and Pyosyn, the latter two being newer synthesis frameworks (Chen et al., 2019; Friedler et al., 2019; Kravanja and Grossmann, 1990; Tian et al., 2018). Most of these frameworks employ MINLP or Generalized Disjunctive Programming (GDP) formulations, using GAMS as mathematical modeling software. They conclude that while there are already many approaches, a fully open-source code and implementation of a general superstructure modeling framework is lacking (Mencarelli et al., 2020). Such an open-source framework would enable the scientific and industry community to develop together and to benefit from each other.

To answer this call for an open-source tool, this paper presents a generic superstructure modeling approach for bi-criteria design optimization. The program code will be fully open and accessible via GitHub. The model code is implemented in the ***O**pen s**U**perstruc**T**ure mo**D**eling and **O**ptimizati**O**n f**R**amework* (OUTDOOR), which is also available on GitHub. The OUTDOOR tool is written in Python using object-oriented programming and follows a modular principle. The OUTDOOR core module creates a superstructure object which is populated by unit-operation objects of different classes such as stoichiometric reactors or stream splitters. This way data can be stored in an intuitive object-oriented way. The stored data is afterwards converted into readable sets, parameters and indices using different programming translation functions. The created data file is then handed to the mathematical model, solved and results are displayed to the user. The model is written utilizing the Python-based, open-source optimization modeling language (PYOMO) and formulated as an object of the abstract model class. It is formulated as a MILP and based on mass, energy and cost balances.

This paper is structured as followed: First, the entire model as implemented in OUTDOOR is described in chapter 2. Afterwards a case study simulating a Power-to-Methanol process is presented in chapter 3. Here design optimization results for a bi-criteria optimization regarding total production costs and total global warming potential are presented. Finally, a conclusion is presented.

2. Methodology

The mathematical model is designed for a generic usability. An important criterion is that the model is formulated in such way that it can be applied to a wide range of applications (e.g. in biorefineries or power-to-x processes). Its basic functionality is the bi-criteria optimization of process design. In this chapter, first the objective functions are described, then the model is described in detail. It should be noted that some equations are only valid for certain unit-operations. Therefore, a detailed look into sets and sub sets has to be taken.

2.1. Objective functions

Two objective functions are defined for this modeling framework, which are depicted in Eq. (1) and (2). The first represents an economic metric. The total annualized costs (*TAC*) are calculated from the total annualized capital costs (*CAPEX*) as well as the total annual operational costs (*OPEX*) and a credit in form of sold byproducts (*PROFITS*).

The total annualized global warming potential of production (*GWP*), i.e. a dedicated environmental impact, represents the second objective function. The induced *GWP* is derived from directly emitted greenhouse gases ($GWP^{EMITTED}$) as well as indirectly induced emissions from external electricity and heat ($GWP^{EL} + GWP^{HEAT}$). The procedure is limited to cradle-to-gate system boundaries and inspired by the life cycle assessment approach. Not included are emissions arising through construction of buildings, as well as supply and transport of raw materials. The corresponding data are often hard to obtain and their contribution

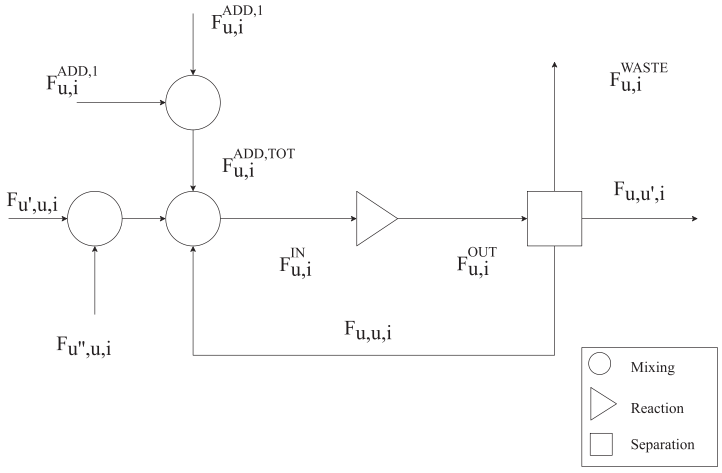

Fig. 1. Mass balance concept for a generic unit-operation u ∈ U (e.g. a stoichiometric/ yield reactor or stream splitter).

to the GWP is usually negligible. The total *GWP* is reduced by captured emissions $GWP^{CAPTURE}$ and credits achieved by the avoided burden approach known from the life-cycle assessment methodology (Horne et al., 2009).

$$\min TAC = CAPEX + OPEX - PROFITS \tag{1}$$

$$\min GWP = GWP^{EMITTED} + GWP^{EL} + GWP^{HEAT} - GWP^{CAPTURE} - CREDITS \tag{2}$$

2.2. Mathematical model

In order to calculate the *TAC* and *GWP*, a mathematical model based on mass and energy balances as well as cost functions for equipment, utilities, raw materials and other expenses is needed.

2.2.1. Mass balance

The superstructure is built by the definition and interaction of different unit-operations (indexed as u ∈ *U)* such as reactors and stream splitters. The foundation of these unit-operations are their mass balances, which are formulated in a generic way according to Fig. 1. Based on the mass balances, energy demands, costs as well as equipment sizes and emissions are calculated for the different unit-operations. In the following, the general mass balance concept is elaborated.

The input of a specific unit-operation u is defined by all feed streams $F_{u',u,i}$ from other unit-operations *u'*, as well as added components $F_{u,i}^{ADD,TOT}$ (cf. Eq. (3)). Here $F_{u,i}^{ADD,TOT}$ is defined as the sum of two process specific added flows $F_u^{ADD_{1/2}}$ with predefined concentrations $\rho_{u,i}^{1/2}$. Eq. (4a) to 4c) show the calculation of total added components. They are written as a Big-M constraint using an upper bound parameter α and a binary decision variable Y_u. This is done to ensure, that only process units that are chosen have a positive added flow, while non-chosen units have a flow of zero. The Big-M formulation is used to keep the model linear. Sometimes, added flows display restricted inputs, meaning only a certain amount of input is available. For this, Eq. (5) and ((6) place constraints of upper limits (*ul*) on added flows.

In some process units, certain concentrations CON_u have to be met. This is ensured by Eq. (7). Depending on the process either the inlet or the outlet flow of different components of the process is used as basis for a required concentration. Using PYOMO as algebraic modeling language it is possible to benefit from the Python conditional programming abilities. This way the choice of input or output flow is done by if-statement programming. Every unit *u* holds parameters of $\kappa_u^{2,lhs}$and $\kappa_u^{2,rhs}$, which are either 0 if the output flow has to be considered, 1 if the input flow hast to be considered or 3 if no flow at all is important (visualized by the curved brackets in Eq. (7)). In addition to that, every process holds parameters of $\kappa_{u,i}^{1,lhs}$ and $\kappa_{u,i}^{1,rhs}$ for every component, which are 1 if the component is to be considered for the concentration or 0 if not.

$$F_{u,i}^{IN} = \sum_{u' \in U} F_{u',u,i} + F_{u,i}^{ADD,TOT} \quad u \in U, \quad i \in I \tag{3}$$

$$F_{u,i}^{ADD,TOT} \leq \alpha \cdot Y_u \quad u \in U, \quad i \in I \tag{4a}$$

$$F_{u,i}^{ADD,TOT} \leq F_u^{ADD_1} \cdot \rho_{u,i}^1 + F_u^{ADD_2} \cdot \rho_{u,i}^2 + \alpha \cdot (1 - Y_u) \quad u \in U, \ i \in I \tag{4b}$$

$$F_{u,i}^{ADD,TOT} \leq F_u^{ADD_1} \cdot \rho_{u,i}^1 + F_u^{ADD_2} \cdot \rho_{u,i}^2 + \alpha \cdot (1 - Y_u) \quad u \in U, \ i \in I \tag{4c}$$

$$F_u^{ADD_1} \leq ul_u^1 \quad u \in U \tag{5}$$

$$F_u^{ADD_2} \leq ul_u^2 \quad u \in U \tag{6}$$

$$\sum_{i \in I} \begin{Bmatrix} F_{u,i}^{OUT} \\ F_{u,i}^{IN} \end{Bmatrix} \cdot \kappa_{u,i}^{1,lhs} = CON_u \cdot \sum_{i \in I} \begin{Bmatrix} F_{u,i}^{OUT} \\ F_{u,i}^{IN} \end{Bmatrix} \cdot \kappa_{u,i}^{1,rhs} \quad u \in U \tag{7}$$

Based on the inlet flows and the type of process, the outlet flows $F_{u,i}^{OUT}$ are calculated. This is done either for stoichiometric or no reactions using Eq. (8a). $\gamma_{i,r,u}$ are stoichiometric factors of component *i*, in reaction *r* and unit *u*, $\theta_{m,r,u}$ are conversion factors of reactant *m*, in reaction *r* and unit *u* and $F_{u,m}^{IN}$ is the inlet flow of reactant *m*. If the process is not a reactor but a simple splitter unit, stoichiometric factors and conversion factors are set to zero. Therefore, the outlet flow is equal to the inlet flow. If the process unit is modeled as a yield-reactor, the outlet flow is calculated using Eq. (8b), where $\zeta_{u,i}$ are yield coefficients of component *i* in unit *u*.

$$F_{u,i}^{OUT} = F_{u,i}^{IN} + \sum_{r \in R, \ m \in M} \gamma_{i,r,u} \cdot \theta_{m,r,u} \cdot F_{u,m}^{IN}$$
$$u = \left\{ u \in U \mid u \notin U^{YIELD} \right\}, \quad i \in I \tag{8a}$$

$$F_{u,i}^{OUT} = \zeta_{u,i} \cdot \sum_{i \in I} F_{u,i}^{IN} \quad u \in U^{YIELD}, \quad i \in I \tag{8b}$$

To complete the mass balance, flows that indicate a link between two process units $F_{u,u',i}$ are defined and combined with binary decision variables $Y_{u'}$. These are set to one if process unit u' is activated and set to zero otherwise. To avoid non-linearities these equations are written as Big-M constraints as shown in Eq. (9a) – (9c). $\mu_{u,u',i}$ depicts a predefined split factor of component i going from unit u to unit u'.

$$F_{u,u',i} \geq \mu_{u,u',i} \cdot F_{u,i}^{OUT} - \alpha \cdot (1 - Y_{u'}) \quad u \wedge u' \in U, \quad i \in I \tag{9a}$$

$$F_{u,u',i} \leq \mu_{u,u',i} \cdot F_{u,i}^{OUT} + \alpha \cdot (1 - Y_{u'}) \quad u \wedge u' \in U, \quad i \in I \tag{9b}$$

$$F_{u,u',i} \geq \mu_{u,u',i} \cdot F_{u,i}^{OUT} - \alpha \cdot (1 - Y_{u'}) \quad u \wedge u' \in U, \quad i \in I \tag{9c}$$

All material flows that leave the system boundaries are considered as waste flows $F_{u,i}^{WASTE}$ and summed up to a total waste flow $F_i^{WASTE,TOT}$ using Eq. (10) and (11). The desired capacity of the plant is set by Eq. (12), where the annual capacity is divided by the full load hours (H) per year.

$$F_{u,i}^{WASTE} = F_{u,i}^{OUT} - \sum_{u' \in U} F_{u,u',i} \quad u \in U, \ i \in I \tag{10}$$

$$F_i^{WASTE,TOT} = \sum_{u \in U} F_{u,i}^{WASTE} \quad i \in I \tag{11}$$

$$\sum_{i \in I} F_{u,i}^{IN} = \frac{F^{PROD}}{H} \quad u = \left\{ u \in U^{PP} \mid u = Main\ Pool \right\} \tag{12}$$

2.2.2. Heat integration

The supply of heating and cooling utilities can be dealt with in different ways. The most detailed approach is an extensive heat exchanger network (HEN) optimization, e.g. using the transshipment model method (Ciric and Floudas, 1991; Kong and Shah, 2017; Yee and Grossmann, 1990)(Yee et al., 1990). However, rigorous HEN optimization using MINLP models is computationally expensive. Since we aim for early design phase superstructure optimization, it is not practical to invest extensive resources for a detailed HEN optimization, while other aspects, such as capital cost calculations are based on simpler concepts. Hence, the rigorous HEN optimization concepts are simplified in this approach in order to keep the model linear, whilst giving initial estimates on heat integration.

Prior to optimization, the required heat integration data must be prepared. This is automated inside OUTDOOR using object-oriented programming. During data preparation, first heating and cooling demands of the different processes are specified by energy demands $\tau_u^{HEAT,1/2}$and $\tau_u^{COOL,1/2}$, as well as given inlet and outlet temperatures. Every process can require up to two heating or cooling demands. This allows for the usage of bigger surrogate models, where different unit-operations (some exothermic others endothermic) are combined into one surrogate unit-operation. It is not necessary to use this feature, but due to the reduced data input, it can come in handy if large superstructures are investigated. Next, OUDOOR defines a temperature grid with fixed heat intervals using the inlet and outlet temperatures of the processes as well as predefined utility temperatures as shown in Fig. 2. Although it is possible to implement different utilities, it is important to implement at least one hot utility whose temperature can satisfy the heat demand of the unit-operations as well as one cold utility which is able to cool down remaining waste heat. To keep the heat integration simple, it is assumed that only the heat of vaporization is used from external steam.

Based on the temperature grid and the predefined specific energy demand, OUTDOOR partitions the required heating and cooling between the heat intervals as shown in Fig. 2. and Eq. (13a) and (13b.) If the process u is a non-isothermal process the ratio $\beta_{u,hi}^H$ is calculated using Eq. (13a), however if the process is designed as an isothermal process ($\Delta T_u = 0$) the ratio for the heat interval of the corresponding temperature is set to 1, using Eq. (13b).

$$\beta_{u,hi}^H = \frac{(T_{hi-1} - T_i)}{\Delta T_u} \quad u \in U, \ hi \in HI \tag{13a}$$

$$\beta_{u,hi}^H = 1 \quad u = \{ u \in U \mid u = Isothermal \}, \ hi \in HI \tag{13b}$$

The data preparation in terms of heat interval based heating and cooling requirement, as described before, is detached from the actual optimization model. OUTDOOR calculates the heat interval-based heat ratios $\beta_{u,hi}^H$ prior to the optimization and feeds it as a parameter to the model itself.

Using the specific heat demand, the heat interval ratio $\beta_{u,hi}^H$ and a specific flow M_u^{HEAT} the cooling demand $Q_{u,hi}^C$ and the heating demand $Q_{u,hi}^H$ of process unit u is calculated using Eq. (14) and (15). Here the specific flow is determined using a similar approach as in the concentration calculation (ref. Eq. (16)).

$$Q_{u,hi}^H = \tau_u^{HEAT,1} \cdot M_u^{HEAT} \cdot \beta_{u,hi}^H + \tau_u^{HEAT,2} \cdot M_u^{HEAT} \ \beta_{u,hi}^{H2} \quad u \in U, \ hi \in HI \tag{14}$$

$$Q_{u,hi}^C = \tau_u^{COOL,1} \cdot M_u^{HEAT} \cdot \beta_{u,hi}^H + \tau_u^{COOL,2} \cdot M_u^{HEAT} \ \beta_{u,hi}^{H2} \quad u \in U, \ hi \in HI \tag{15}$$

$$M_u^{HEAT} = \begin{cases} \sum_{i \in I} \begin{cases} F_{u,i}^{OUT} \\ F_{u,i}^{IN} \\ E_u^{EL} \end{cases} \cdot \kappa_{el,\ u,i}^{1,\ ut} & u \in U \end{cases} \tag{16}$$

Additionally, to the interval-based heating and cooling demand, some unit-operations are labeled as steam generators. These units burn combustible components to produce heat at the highest defined temperature interval, generally superheated steam. The usable heat is calculated by the lower heating value LHV_i and an efficiency coefficient η_u^{HEAT} (cf. Eq. (17)). This superheated steam can be used internally or sold to the market, realized by Eq. (18).

$$Q_u^{PROD} = \eta_u^{HEAT} \cdot \sum_{i \in I} F_{u,i}^{IN} \cdot LHV_i \quad u \in U^{HEATGEN} \tag{17}$$

$$Q^{PROD,USE} = \sum_{u \in U^{HEATGEN}} Q_u^{PROD} - Q^{PROD,SELL} \tag{18}$$

Based on the calculated heating and cooling demands as well as the produced superheated steam, the energy balances are written for every heat interval for the heating site as shown in Eq. (19a) and (19b) as well as the cooling site as given in Eq. (20a) – (20c).

$$\sum_{u \in U} Q_{u,hi}^H - Q_{hi}^{DEFI} - Q_{hi}^{EX} = 0 \quad hi = \left\{ hi \in HI \mid hi \neq HI^{LP} \right\} \tag{19a}$$

$$\sum_{u \in U} Q_{u,hi}^H - Q_{hi}^{DEFI} - Q_{hi}^{EX} - Q^{HP,USE} = 0 \quad hi = HI^{LP} \tag{19b}$$

Q_{hi}^{DEFI}depicts the heat deficit of interval hi which cannot be supplied by exchanged heat Q_{hi}^{EX}. For hot streams, residual heat Q_{hi}^{RESI} is calculated at each interval. This heat can be cascaded down to intervals with lower temperatures. On the heat interval with the

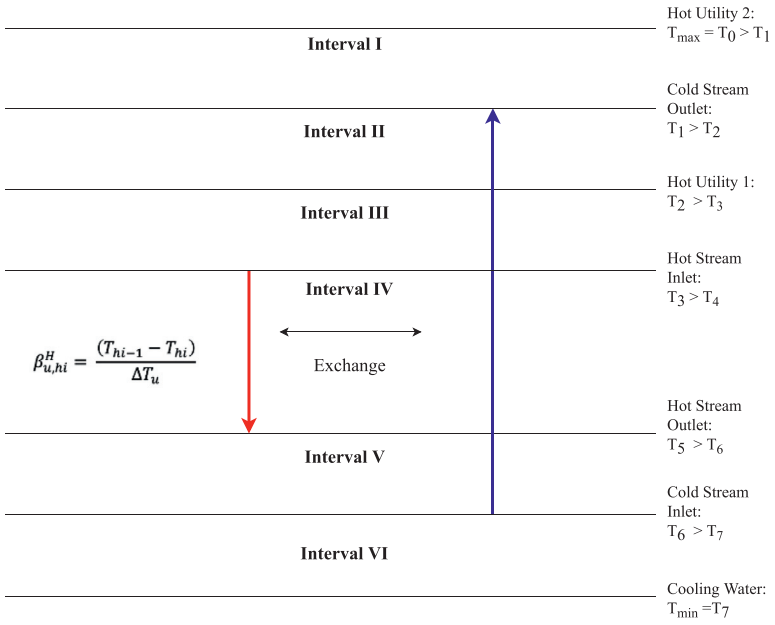

Fig. 2. Example representation of the temperature grid with heat intervals.

lowest temperature (interval HI^M) heat surplus can either be used in the heat pump if required to produce low pressure steam (Q^{HP}) or has to be cooled down by utilizing cooling water (Q^{COOL}).

$$\sum_{u \in U} Q^{C}_{u,hi} - Q^{RESI}_{hi} - Q^{EX}_{hi} + Q^{PROD,USE} = 0 \quad hi = 1 \tag{20a}$$

$$\sum_{u \in U} Q^{C}_{u,hi} - Q^{RESI}_{hi} - Q^{EX}_{hi} + Q^{RESI}_{hi-1} = 0$$
$$hi = \left\{ hi \in HI \mid hi \neq 1 \ \vee \ HI^M \right\} \tag{20b}$$

$$\sum_{u \in U} Q^{C}_{u,hi} + Q^{RESI}_{hi-1} - Q^{EX}_{hi} - Q^{COOL} - Q^{HP} = 0 \quad hi = HI^M \tag{20c}$$

The exchanged heat at each interval hi has to be lower or equal to the sum of required cooling and internally utilized superheated steam as well as the sum of required heating for the heat interval at highest temperatures. For all other intervals the exchanged heat has to be lower or equal to the required cooling plus the residual heat and lower than the required heating (cf. Eq. (21a) – (21c)). In addition, a binary variable Y^{HEX}_{hi} is introduced to distinguish between heat intervals chosen for heat exchange and those who are not (ref. Eq. (22)).

$$Q^{EX}_{hi} \leq \sum_{u \in U} Q^{C}_{u,hi} + Q^{PROD,USE} \quad hi = 1 \tag{21a}$$

$$Q^{EX}_{hi} \leq \sum_{u \in U} Q^{H}_{u,hi} \quad hi \in HI \tag{21b}$$

$$Q^{EX}_{hi} \leq \sum_{u \in U} Q^{C}_{u,hi} + Q^{RESI}_{hi-1} \quad hi = \{ hi \in HI \mid hi \neq 1 \} \tag{21c}$$

$$Q^{EX}_{hi} \leq Y^{HEX}_{hi} \cdot \alpha^{HEX} \quad hi \in HI \tag{22}$$

This heat integration framework provides a way to implement a high temperature heat pump, which uses low exegetic heat as well as electricity for generation of low-pressure steam. The ratio of usable steam $Q^{HP,USE}$ and utilized low-ex heat Q^{HP} is determined by the coefficient of performance COP^{HP} as expressed in Eq. (23).

$$Q^{HP,USE} = \frac{Q^{HP}}{1 - \left(1 - COP^{HP}\right)} \tag{23}$$

2.2.3. Electricity balances

Besides heating and cooling, electricity is the second utility required in many processes. If electricity is consumed in unit-operation u, the demand is calculated using a specific electricity demand τ^{EL}_u and a corresponding unit specific flow M^{EL}_u (ref. Eq. (24)), similar to the calculation of heating and cooling demand. The specific reference flow is defined by either the outlet or the inlet flow of a series of components determined by the binary parameter $\kappa^{1,\ ut}_{el,\ u,i}$, similar to the concentration calculation (Eq. (25)). If the unit u is labeled as an electricity generation unit, e.g. a combined power circle process, the produced electricity is calculated using a process efficiency η^{EL}_u together with the lower heating values LHV_i of the entering compounds as depicted in Eq. (26). In addition to unit-operation specific electricity demand and generation, further electricity demand can be generated if a high-temperature heat pump is utilized for heat integration. This demand depends on the COP and the provided steam, as shown in Eq. (27). The total demand of external purchased electricity is determined by the total demand of the process units as well as the demand of the heat pump minus by the onsite produced electricity (see Eq. (28)).

$$E^{EL}_u = \tau^{EL}_u \cdot M^{EL}_u \quad u \in U \tag{24}$$

$$M^{EL}_u = \sum_{i \in I} \begin{cases} F^{OUT}_{u,i} \\ F^{IN}_{u,i} \end{cases} \cdot \kappa^{1,\ ut}_{el,\ u,i} \tag{25}$$

$$E^{EL,PROD}_u = \eta^{EL}_u \cdot \sum_{i \in I} F^{IN}_{u,i} \cdot LHV_i \quad u \in U^{ELGEN} \tag{26}$$

$$E^{EL,HP} = \frac{Q^{HP}}{\left(COP^{HP} - 1\right)} \tag{27}$$

$$E^{EL,TOT} = \sum_{u \in U} E^{EL}_u + E^{EL,HP} - \sum_{u \in U^{ELGEN}} E^{EL,PROD}_u \tag{28}$$

2.2.4. Cost functions

The total annualized capital costs (*CAPEX*) are calculated based on major equipment costs (EC_u). These costs are in general nonlinear depended on the capacity of a unit u. Using economy of scale and a reference plant, costs can be calculated using Eq. (29).

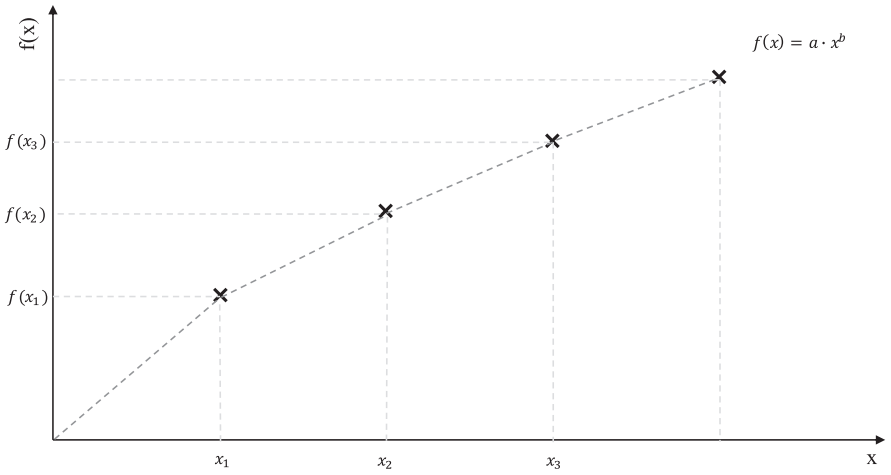

Fig. 3. Example of Piece-wise linearized function.

The specific flow M_u^{CAPEX} is again determined during the calculation, using Eq. (30).

$$EC_u^{Non-linear} = C_u^{REF} \left(\frac{M_u^{CAPEX}}{M_u^{REF}} \right)^{f_u} \cdot \frac{CECPI}{CECPI_u^{REF}} \quad u \in U^C \tag{29}$$

$$M_u^{CAPEX} = \begin{cases} \sum\limits_{i \in I} \begin{cases} F_{u,i}^{OUT} \\ F_{u,i}^{IN} \end{cases} \cdot \kappa_{u,i}^{1,\ capex} \\ E_u^{EL} \\ Q_u^{PROD} \\ E_u^{EL,PROD} \end{cases} \quad u \in U^C \tag{30}$$

However, the economies of scale are non-linear and can therefore pose serious computational issues in solving, especially for large superstructures with many unit-operations. In order to reduce the complexity of the model, the economies of scale equations can be linearized using piece-wise formulation and lambda-constraint programming, as presented in Eq. (31) and (32) (Bisschop, 2016).

$$M_u^{CAPEX} = \sum_{k \in K} \lambda_{k,u} \cdot x_{k,u} \quad u \in U^C \tag{31}$$

$$EC_u = \sum_{k \in K} \lambda_{k,u} \cdot f(x)_{k,u} \quad u \in U^C \tag{32}$$

$$\sum_{k \in K^I} z_{u,k}^{CAPEX} = 1 \quad u \in U^C \tag{33}$$

$$s_{u,k}^{CAPEX} \leq z_{u,k}^{CAPEX} \quad u \in U^C,\ k \in K \tag{34}$$

$$\lambda_k = z_{u,k}^{CAPEX} - s_{u,k}^{CAPEX} \quad u \in U^C,\ k = 1 \tag{35a}$$

$$\lambda_k = s_{u,k-1}^{CAPEX} \quad u \in U^C,\ k = K^M \tag{35b}$$

$$\lambda_k = z_{u,k}^{CAPEX} - s_{u,k}^{CAPEX} + s_{u,k-1}^{CAPEX} \quad u \in U^C,\ k = \left\{ k \in K \mid k \neq 1 \vee K^M \right\} \tag{35c}$$

Here $x_{k,u}$ and $f(x)_{k,u}$ represent pre-calculated reference flows M_u^{REF} and equipment costs $EC_u^{Non-linear}$ of linear interval k, as shown in Fig. 3. Eq. (33) – (35c) illustrate the implementation of special ordered sets type 2 as presented in (Morrison, 2008).

Using the calculated major equipment costs, first the fixed capital investment (FCI_u) is determined by linear cost factors for direct (installation, electrics etc.) as well as indirect costs (engineering, legal costs, insurance) (ref. Eq. (36)). Afterwards the annualized capital costs (ACC_u) are computed using a capital recovery factor (f_u^{ACC}) which is determined beforehand for each process unit to avoid non-linearities (cf. Eq. (37) and (38)).

$$FCI_u = EC_u \cdot \left(1 + f_u^{DC} + f_u^{IDC}\right) \quad u \in U^C \tag{36}$$

$$ACC_u = FCI_u \cdot f_u^{ACC} \quad u \in U^C \tag{37}$$

$$f_u^{ACC} = \frac{IR \cdot (1+IR)^{LT}}{(1+IR)^{LT} - 1} \quad u \in U^C \tag{38}$$

Some major equipment have regular recurring investment costs, such as catalysts or electrolysis stacks which must be replaced every 3-5 years, or 40,000-60,000 full load hours instead of every 20 years. These costs are considered as repeating recurrence costs ACC_u^{RE} (ref Eq. (40)). These costs are calculated as a function from the required number of periods n_u^{RE} during the lifetime of a unit-operation and a percentage c_u^{RE} of the raw purchase equipment costs. The number of periods is dependent on the lifetime of the unit-operation as well as the frequency of replacement, which is either given on hourly basis ($LT_u^{RE,h}$) or on yearly basis ($LT_u^{RE,y}$) (Eq. (39)). The second case is more relevant if the plant is operated with low occupancy rate.

$$n_u^{RE} = \begin{cases} LT_u / LT_u^{RE} \\ LT_u \cdot H / LT_u^{RE,h} \end{cases} \quad u \in U^C \tag{39}$$

$$ACC_u^{RE} = c_u^{RE} \cdot n_u^{RE} \cdot EC_u \cdot f_u^{ACC} \quad u \in U^C \tag{40}$$

In addition to the costs derived from the major equipment, the capital costs for the heat integration have to be considered. Here two factors have to be calculated. The capital costs for the high temperature heat pump, as well as the heat exchanger network (HEN) itself.

The costs for the heat pump are derived from Eq. (41), using the heat supplied by the heat pump as well as a capital recovery factor $f^{ACC,HP}$ and specific costs per kW installed (EC^{HP}).

$$ACC^{HP} = Q^{HP,USE} \cdot f^{ACC,HP} \cdot EC^{HP} \tag{41}$$

The costs of the HEN are calculated using a simplified approach of the major equipment cost calculation for heat exchangers. Here, it is assumed, that the costs of the simplified HEN are reflected by the costs of one big heat exchanger per heat interval. The costs

of the heat exchanger (HEX) are dependent on its heat duty (cf. Eq. (42a) – (42c)). Linearized reference costs of a comparative HEX were calculated beforehand using Aspen Plus simulation, resulting in slope m^{HEN} and axis intercept b^{HEN}. To only consider heat exchangers that exchange heat, the costs are derived using the defined binary variable Y_{hi}^{HEX}, written as a Big-M constraint. The total annualized capital expenditures (*CAPEX*) are defined by the sum of all annualized capital costs (ref. Eq. (43)).

$$ACC_{hi}^{HEN} \leq m^{HEN} \cdot Q_{hi}^{EX} + b^{HEN} + \alpha^{HEX} \cdot \left(1 - Y_{hi}^{HEX}\right) \quad hi \in HI \tag{42a}$$

$$ACC_{hi}^{HEN} \geq m^{HEN} \cdot Q_{hi}^{EX} + b^{HEN} - \alpha^{HEX} \cdot \left(1 - Y_{hi}^{HEX}\right) \quad hi \in HI \tag{42b}$$

$$ACC_{hi}^{HEN} \leq \alpha^{HEX} \cdot Y_{hi}^{HEX} \quad hi \in HI \tag{42c}$$

$$CAPEX = \sum_{u \in U^C} ACC_u + ACC^{HP} + \sum_{hi \in HI} ACC_{hi}^{HEN} + \sum_{u \in U^C} ACC_u^{RE} \tag{43}$$

The operational costs (*OPEX*) are derived from utility costs, raw material costs as well as costs for operation and maintenance of the process plant. The electricity costs are calculated from the total electricity demand of the system and the specific electricity price δ^{EL} Eq. (44)). The costs for heating are derived from the heat deficit at the different intervals and the external purchase costs of steam δ_{hi}^{H}, while sold steam is vended for 70 % of the purchase costs. Cooling costs are dependent on the cooling demand and costs for cooling water respectively (Eq. (45) and ((46)). The total costs of utilities are the sum of electricity, heating and cooling costs (Eq. (47)).

$$C^{EL} = \left(E^{EL,TOT} + E^{EL,HP}\right) \cdot \delta^{EL} \cdot H \tag{44}$$

$$C^{HEAT} = \left(\left[\sum_{hi \in HI} Q_{hi}^{DEFI}\right] + Q^{PROD,SELL} \cdot 0.7 \cdot \delta_{hi=1}^{H}\right) \cdot H \tag{45}$$

$$C^{COOLING} = Q^{COOL} \cdot \delta^{COOL} \cdot H \tag{46}$$

$$C^{UT} = C^{HEAT} + C^{EL} + C^{COOLING} \tag{47}$$

Costs for raw materials are derived from the added Flows $F_{u,i}^{ADD,TOT}$ with their respective costs of components δ_i^{RM} (Eq. (48a) – (48c) and (49)).

$$C_u^{RM} \leq \alpha \cdot Y_u \quad u \in U \tag{48a}$$

$$C_u^{RM} \leq \left[\sum_{i \in I} F_{u,i}^{ADD,TOT} \cdot \delta_i^{RM}\right] + \alpha \cdot (1 - Y_u) \quad u \in U \tag{48b}$$

$$C_u^{RM} \geq \left[\sum_{i \in I} F_{u,i}^{ADD,TOT} \cdot \delta_i^{RM}\right] - \alpha \cdot (1 - Y_u) \quad u \in U \tag{48c}$$

$$C^{RM,TOT} = \sum_{u \in U} C_u^{RM} \cdot H \tag{49}$$

The costs for operating and maintenance are determined in two steps. The maintenance costs are the sum of the fixed capital investment multiplied by a process specific maintenance factor f_u^M (Eq. (50)). The operating costs are related to the workings hours (WH), a factor which takes overhead, materials etc. into account (f^O) and the hourly wage (c^{Labor}) (ref. Eq. (52)) (Albrecht et al., 2017). Thereby, the working hours are a parameter derived beforehand based on the capacity of the plant, the number of major process steps and the operating days per year (Eq. (51)).

$$C^M = \sum_u f_u^M \cdot FCI_u \tag{50}$$

$$WH = 2.13 \cdot \left(\frac{F^{PROD}}{H \cdot 1000}\right)^{0.242} \cdot n^{PS} \cdot \frac{H}{24} \tag{51}$$

$$C^O = f^O \cdot WH \cdot c^{Labor} \tag{52}$$

$$C^{O\&M} = C^M + C^O \tag{53}$$

The total operating costs are the sum of utility costs, costs for raw materials as well as operating and maintenance costs $C^{O\&M}$ (Eq. (54)). In addition to the costs, revenues can also be generated. These are determined by the total inlets of the defined product pools with their respective market prices (Eq. 55).

$$OPEX = C^{O\&M} + C^{UT} + C^{RM,TOT} \tag{54}$$

$$PROFITS = \sum_{u \in U^{PP}} \left(\sum_{i \in I} F_{u,i}^{IN}\right) \cdot \delta_u^{PP} \cdot H \tag{55}$$

2.2.5. Emission functions

Emissions that induce global warming can be directly emitted at the plant ($GWP^{EMITTED}$). These are calculated from the waste flows with their respected global warming potential factor (gwp_i), (Eq. (56)).

$$GWP^{EMITTED} = \sum_{u \in U} \sum_i F_{u,i}^{WASTE} \cdot gwp_i \cdot H \tag{56}$$

However, they can also emerge as indirect emissions from external utility supply. These are derived from the usage of external utilities, such as electricity from the energy grid or renewable sources and steam produced from natural gas (cf. Eq. (57) and (58)).

$$GWP^{EL} = \left(E^{EL,TOT} \cdot gwp^{Electricity}\right) \cdot H \tag{57}$$

$$GWP^{HEAT} = \left(\left[\sum_{hi \in HI} Q_{hi}^{DEFI}\right] - Q^{PROD,SELL}\right) \cdot gwp^{Heat} \cdot H \tag{58}$$

Negative emissions can be achieved by captured CO_2 as depicted in Eq. (59) or by CREDITS for byproducts according to the avoided burden approach (Horne et al., 2009). These credits are calculated using the inlet flow of the given product pools with their respective reference gwp value (Eq. (60)). This approach requires knowledge of reference production processes (e.q. oxygen from air separation) as well as the assumption that by-products can be sold and therefore lead to avoided burden.

$$GPW^{CAPTURE} = \sum_{u \in U} \left(\sum_{i \in I} F_{u,i}^{ADD,TOT} \cdot gwp_i\right) \cdot H \tag{59}$$

$$CREDITS = \sum_{u \in U^{PP}} \sum_{i \in I} F_{u,i}^{IN} \cdot gwp_u^{avoided} \tag{60}$$

Table 1
Assumptions on key parameters (Albrecht et al., 2017; Methanex 2019; Wassermann et al., 2020; Wernet et al., 2016).

Parameter	Value	Unit	Parameter	Value	Unit
Full load hours (H)	4000	h/y	Oxygen price	26.3	€/t
Interest rate	0.05	-	Waste water costs	3.8	€/t
Costs of electricity	50	€/MWh	COP^{HP}	3	-
Electricity emissions	0.015	$t_{CO2\text{-}eq.}$ /MWh	ASU emissions	0.585	$t_{CO2\text{-}eq}$ / t_{O2}
Steam emissions	0.248	$t_{CO2\text{-}eq.}$ /MWh	Product load	200	kt_{MeOH} / y
MEA price	1450	€/t	H_2O price	2	€/t
Conventional methanol emissions	0.586	$t_{CO2\text{-}eq.}$ /t_{MeOH}	Conventional methanol costs	325	€/t
HP COP	2.5	-	HP Costs	450	€/kW
HP T_{IN}	65-75	°C	HP T_{OUT}	130	°C

Table 2
Heating and cooling utility characteristics (SH = Superheated, HP = High pressure, MP = Medium pressure, LP = Low pressure, CW = Cooling water).

Utility	SH Steam	HP Steam	MP Steam	LP Steam	CW
Temperature	600°C	330°C	220°C	130°C	15°C
Costs [€/MWh]	34	32	30	29	0.22

3. Case study

The presented model is applied to a Power-to-Methanol case study. First, the case study is described, afterwards the resulting model is characterized and results for bi-criteria optimization are presented. It should be noted that while some data is obtained by process simulation for this specific case study, this is not inherently necessary. In addition to generating input data using commercial or open-source process simulators such as Aspen Plus or DWSIM, it can also be collected from literature or obtained through discussion with industry.

3.1. General assumptions

The Power-to-Methanol process design is investigated with generic assumptions. However, some relevant data, such as the electricity purchase costs and natural gas costs as well as specific emissions for utilities are inspired by the German energy system. Table 1. shows the corresponding key figures . Full load hours and greenhouse gas emissions associated with electricity supply reflect direct electricity purchase from offshore wind farms. It is assumed that produced oxygen can substitute oxygen from conventional air separation units.

Heating utility costs were calculated using Aspen Plus simulation and the Aspen Plus economy tool. For this purpose, natural gas combustion and cooling via a cascade of four heat exchangers is considered. Thereby, saturated low, medium and high-pressure steam as well as superheated high-pressure steam are produced. Natural gas costs were assumed to be 2.785 ct/kWh based on costs for German industry (Statista 2020). These costs as well as the costs for the combustor were allocated to all four steam types, while the costs of the heat exchangers were only allocated to the steam type they produced. Cooling utility costs were calculated based on costs for cooling water and heat capacity, assuming maximum permissible temperature differences in Germany when cooling water is taken from a river. Table 2. shows the resulting costs of utilities.

3.2. Power-to-Methanol superstructure

The Power-to-Methanol (PtM) process is composed of four process stages. The first is the acquisition of carbon dioxide as raw material. The second stage presents the acquisition of hydrogen as the second raw material. Together CO_2 and H_2 are reacted to crude methanol in a chemical reactor. Afterwards, the crude methanol is purified using flash drums and distillation columns to separate unreacted offgas and water. The reactor and purification define the third stage of the PtM process. The last stage depicts the handling of wastes and recycles. The separated offgas still consists of highly energetic gases like H_2 and CO and traces of methanol. These gases can be burned and either used for production of steam or electricity.

Fig. 4. shows the complete superstructure with its four stages and multiple options. In the following, the different process stages will be explained in more detail and the implemented unit-operation options are listed.

3.2.1. Electrolysis

Water electrolysis uses electricity and, in case of a high temperature electrolysis, heat to split water molecules into hydrogen and oxygen molecules. It therefore depicts the hydrogen acquisition process, while producing oxygen as byproduct.

Three different water electrolysis technologies are considered in this superstructure. These are the proton exchange membrane electrolysis (PEMEL), the alkaline electrolysis (AEL) and the solid oxide (high temperature) electrolysis (SOEL). For all three technologies it is assumed, that one kg of water is completely reacted into 0.112 kg of hydrogen and 0.888 kg of oxygen as depicted in Eq. (61).

$$H_2O \rightarrow \ 0.888\ O_2 + 0.112\ H_2 \tag{61}$$

For the PEMEL and AEL two different operating modes are implemented. The first is an atmospheric operation with a consecutive two step pressurization of the hydrogen product to 70 bar. The second mode of operation is a high pressure setting at 30 bar with a single step pressurization to 70 bar. Electrolyzer costs and energy demands were modeled using recent literature leading to electricity demand from 4.4 kWh/Nm^3 to 4.9 kWh/Nm^3 and capital costs from 700 €/$kW_{installed}$ to 3000 €/$kW_{installed}$. (Proost, 2019; Smolinka et al., 2018; Wang et al., 2019)

3.2.2. Carbon capture system

Carbon capture is considered with three different sources. One way to acquire CO_2 is utilizing low temperature direct air capture (DAC) based on the technology provided by Climeworks (Fasihi et al., 2019). Concentrated CO_2 sources are so-called point sources, these are often waste streams which have no value or benefit for their producing factory. In this case study one possible point source is flue gas from a cement factory using oxy-fuel combustion and consecutive chilling and water separation (Gardarsdottir et al., 2019; Voldsund et al., 2019). The other point source is a merged flue gas stream from a catalytic reformer, a steam cracker and a combined heat and power plant of a crude oil refinery. CO_2 is captured using monoethanolamine (MEA) as chemical absorbent, with the flue gas composition depicted in Table 3. (Wassermann et al., 2020).

3.2.3. Methanol synthesis

One option for the methanol synthesis is implemented in the superstructure. This option represents a direct hydrogenation of

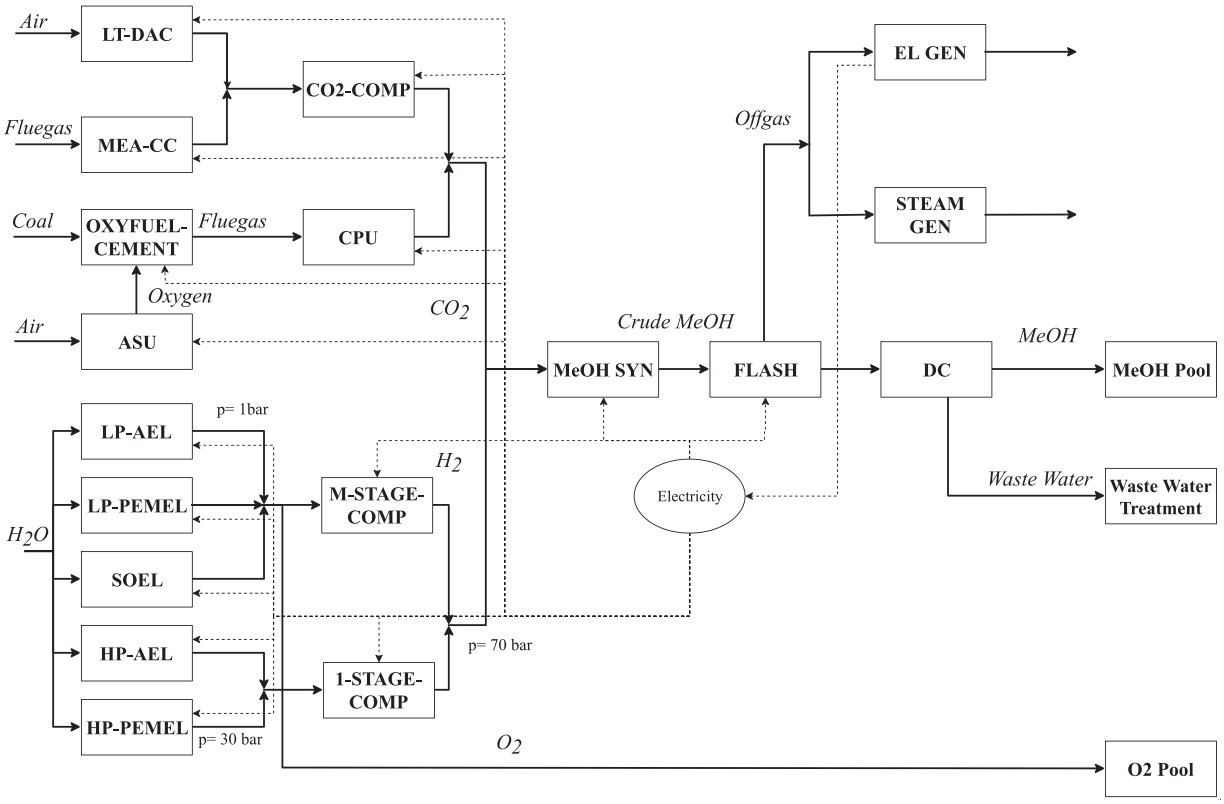

Fig. 4. Superstructure representation of the Power-to-Methanol plant (LT-DAC: Low temperature direct air capture, MEA-CC: Absorption-based CO_2 capture, OXYFUEL-CEMENT: Cement factory oxyfuel combustion, ASU: Air separation unit, CPU: CO_2 purification unit, CO2-COMP: CO_2 Compressor, LP/HP AEL: Ambient / High pressure alkaline electrolysis LP/HP PEMEL: Ambient / High pressure proton exchange membrane electrolysis, SOEL: Solid oxide electrolysis, 1/M - STAGE COMP: Hydrogen compression units, MeOH SYN: Methanol reactor, FLASH: Flash and integrated depressurization with intercooling, DC: Distillation column, EL GEN: Combined Gas and Steam power-plant, STEAM GEN: Furnace).

Table 3
Refinery flue gas composition (Wassermann et al., 2020).

Component	Nitrogen (N_2)	Carbon dioxide (CO_2)	Oxygen (O_2)	Water (H_2O)
Mass-fraction	0.732	0.139	0.041	0.088

Table 4
Yield factors for MeOH Reactor Surrogate Model derived from (Wassermann et al., 2020).

Component	MeOH	CO_2	O_2	H_2O	CO	H_2
Yield Factor	0.619	0.023	0.002	0.35	0.002	0.002

CO_2 at 250°C and 70 bar operating conditions. The synthesis reactor is modeled as a yield reactor with yield coefficients as presented in Table 4. After the methanol synthesis, purification is performed in two unit-operations. The first one depicts a flash drum to separate offgas which is treated downstream. The liquid phase is then further purified by a distillation column to separate water and methanol. The data for equipment costs, utility demand and operating conditions such as split factors, temperature and yield factors is derived from a rigorous model published by (Wassermann et al., 2020).

3.2.4. Offgas treatment

Arising offgases in the methanol reactor still contain some combustible components such as hydrogen, carbon monoxide and rests of gaseous methanol. In order to utilize the its energy, enhance the overall performance of the process and react all unreacted components to CO_2, offgas treatment is considered. This offgas treatment can either be a combustion in order to generate steam for internal heat supply or electricity generation by combustion and utilization of a combined cycle power plant (Gong and You, 2015).

3.2.5. Wastewater treatment

The separated water from the distillation column and water separators still holds some extent of methanol and other hydrocarbons. If this water is to be disposed, it has to be purified. This waste water treatment step is not modeled in detail but it is assumed, that specific costs per ton of water arise through waste water treatment (Albrecht et al., 2017).

3.3. Model characteristics

The presented case study leads to a mixed integer linear program. The number of parameters, continuous and binary variables as well as constraints is highly dependent on the number of linear intervals used in the piece-wise linearization of the equipment costs section. To investigate solver performance two cases are tested. One using a fine linearization with 300 intervals per process unit, and another with a rougher linearization using overall 20 intervals per process unit. The fine configuration leads to a high- detail model with 30,145 constraints and 23,709 variables of which 5,437 were binary. The rough configuration is smaller and leads to a low-detail model of 20,029 constraints and 8,535 variables of which 379 were binary.

Table 5
Key figures fiof the Power-to-Methanol optimization.

Objective	Net present costs ($€/t_{MeOH}$)	Net present emissions ($t_{CO\text{-}eq.}/t_{MeOH}$)	CO_2 abatement costs ($€/t_{CO2\text{-}eq.}$)
Cost optimal PtM	891.94	-1.937	225
Constrained GWP-optimal PtM	978.68	-2.191	235
Unconstrained GWP-optimal PtM	1,17 M	-1157.57	1010

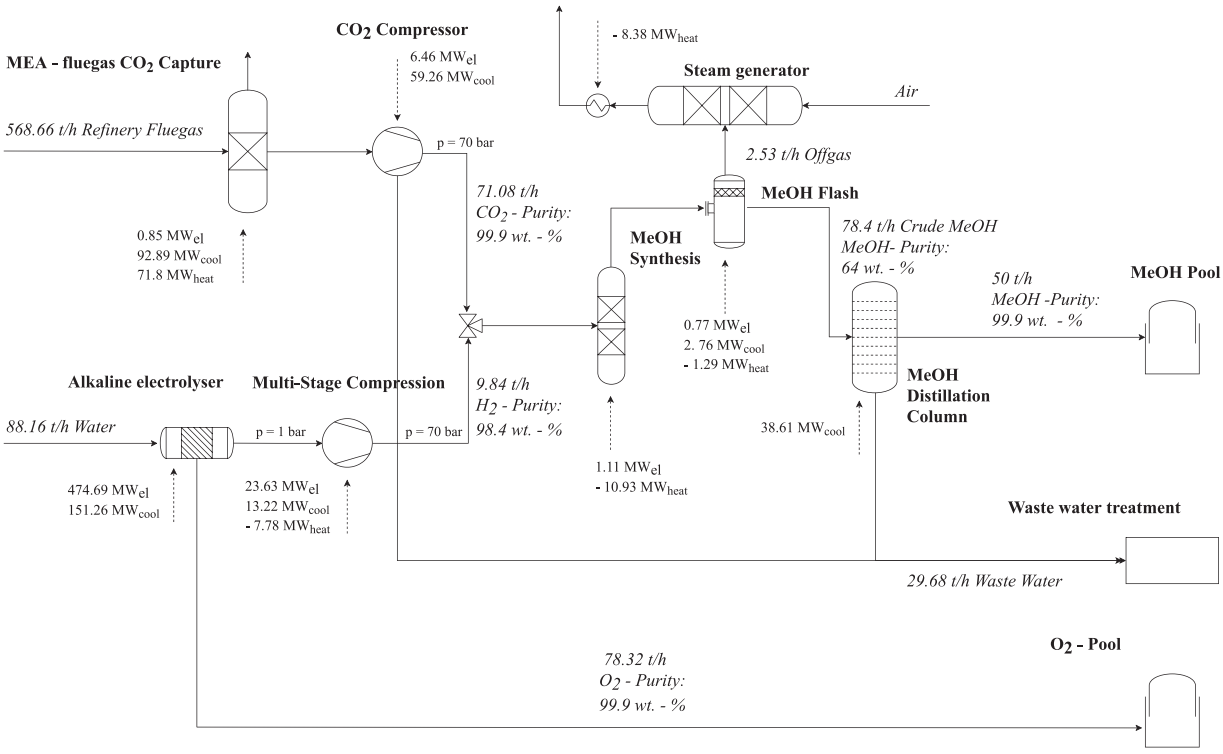

Fig. 5. Process flow-sheet of cost-optimized Power-to-Methanol process.

4. Results and Discussion

4.1. Computational performance

The MILP problem was solved using a MacBook Pro with a 2 GHz Dual-Core Intel Core i5 processor and 8 GB RAM. Different solvers are tested for performance differences. First Cbc as an open-source MILP solver was tested using the low-detail model. Cbc finds an optimal solution after 70 seconds. Afterwards Gurobi as commercial state-of-the art MILP solver is compared to Cbc. Gurobi only takes 4 seconds to find the solution, providing high performance gains. Testing the high-detail model Cbc showed some performance issues, while Gurobi solved the problem in 9 seconds. Due to Cbc's performance issues the high-detail model was also optimized, utilizing Cplex as part of the neos-server (Czyzyk et al., 1998; Dolan, 2001). This configuration requires about 71 seconds while providing the same results as Gurobi. While it seems possible to solve the model with all solvers, the following results were acquired by using Gurobi, for performance reasons while using the high-detail model to gain more accurate results.

4.2. Base case results

Optimization runs were performed for cost-optimal and emission-optimal Power-to-Methanol plant design. Optimization in terms of emissions leads to a plant design that effectively produces renewable oxygen, while discarding most of the hydrogen as waste. Therefore, a third case was calculated, prohibiting the emission of pure hydrogen by an additional constraint. Key findings of the three optimization runs of the base case can be found in Table 5, and will be discussed in more detail in the following sections.

4.2.1. Economic optimization

A cost-optimal Power-to-Methanol plant produces MeOH at costs of about 892 $€/t_{MeOH}$, while avoiding 1.937 $t_{CO\text{-}eq.}/t_{MeOH}$. This results in CO_2 abatement costs of around 225 $€/t_{CO2\text{-}eq.}$. Hydrogen is produced by ambient pressure alkaline electrolysis with a multi-stage compression to 70 bar. The CO_2 is provided by flue gas capture from the refinery using MEA as solvent. The produced offgas in the methanol synthesis step is combusted to produce superheated steam. The flowsheet is depicted in Fig. 5. The exothermal methanol synthesis, as well as intercooling of hydrogen during the multi-stage compression provides heat at high temperature. The heat balance indicates that this heat is integrated in the CO_2 capture process, being sufficient to cover 27.85 % of its heat demand. In addition, heat from offgas combustion provides 11.66 % of the demand, resulting in a total share of 39.51 % of heat satisfied via heat integration. The rest is covered by external low-pressure steam.

A cost breakdown for the cost-optimal process design is provided in Fig. 6. It illustrates that around 54 % of the overall costs

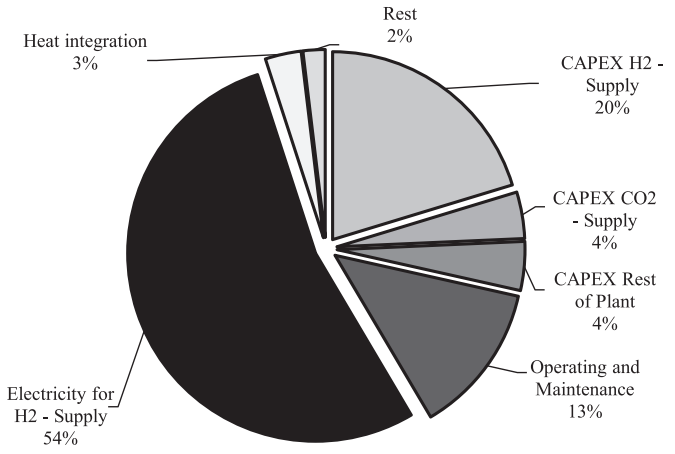

Fig. 6. Cost Breakdown of cost optimal Power-to-Methanol Case.

emerge as electricity costs for the hydrogen supply, while 20 % arise from the capital expenditures for the electrolyser and hydrogen compression unit. Around 13 % of the costs are operating and maintenance costs, which are directly related to the CAPEX of the overall system. It is apparent, that the hydrogen supply contributes over 74 % percent of the overall costs, making it the economic bottleneck of synthetic methanol.

4.2.2. Environmental optimization

An unconstrained environmental optimization leads to oxygen production plant designs. This means, that hydrogen production capacities are increased until numerical limits. While the produced oxygen is sold as product to gain environmental credits, most of the hydrogen is regarded as waste flow. This leads to enormous net production costs of 1.17 million €/t_{MeOH} with minimal net production emissions of -1157 $t_{CO2\text{-}eq.}$ /t_{MeOH}. This behavior can be explained by the avoided burden assigned to the oxygen. The avoided burden is based on oxygen production by air separation units, which are operated with electricity from the German energy grid. Due to the fact, that the Power-to-Methanol plant is operated with wind energy, the oxygen production via. electrolysis is environmental superior to the air separation unit leading to an abnormal oxygen production.

To avoid this effect and to generate results that can be reasonably assessed in the subject of synthetic methanol production, an additional constraint is added to the model. This constraint prohibits the direct emission of hydrogen from electrolysis, thus enforcing the utilization of the produced hydrogen during the methanol synthesis. The corresponding process design can be observed in Fig. 7. It shows higher costs of ca. 979 €/t_{MeOH} with higher CO_2 abatement of -2.191 $t_{CO2\text{-}eq.}$/t_{MeOH}, and slightly higher CO_2 abatement costs of 235 €/$t_{CO2\text{-}eq}$. This design produces hydrogen from low pressure alkaline electrolysis. However, in contrast to the cost-optimal design, carbon dioxide is captured from refinery flue gas via. absorption only to the point until the exothermal potential of the methanol synthesis is depleted, while further low temperature heat at about 100°C is utilized for direct air cap-

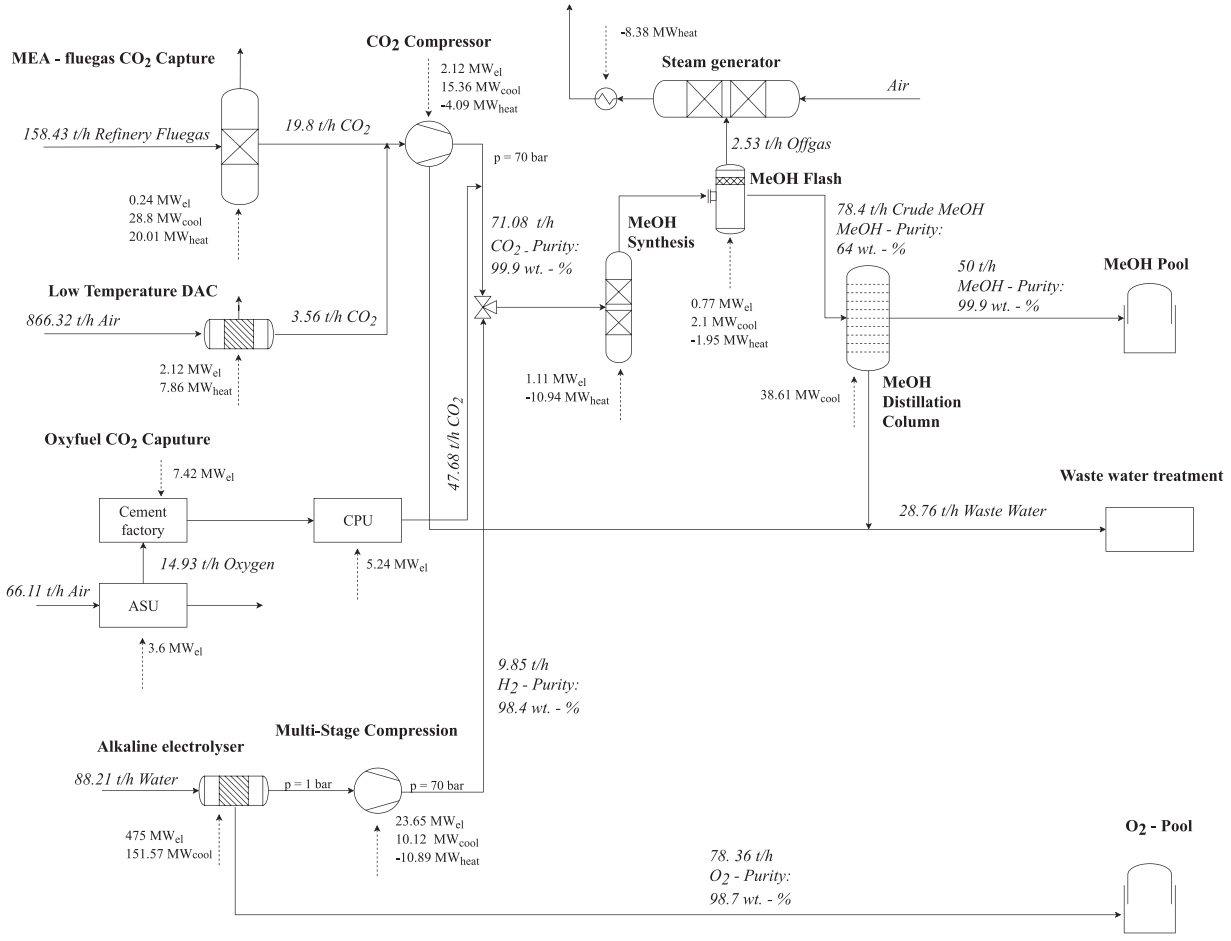

Fig. 7. Process flowsheet of the environmentally optimized Power-to-Methanol process.

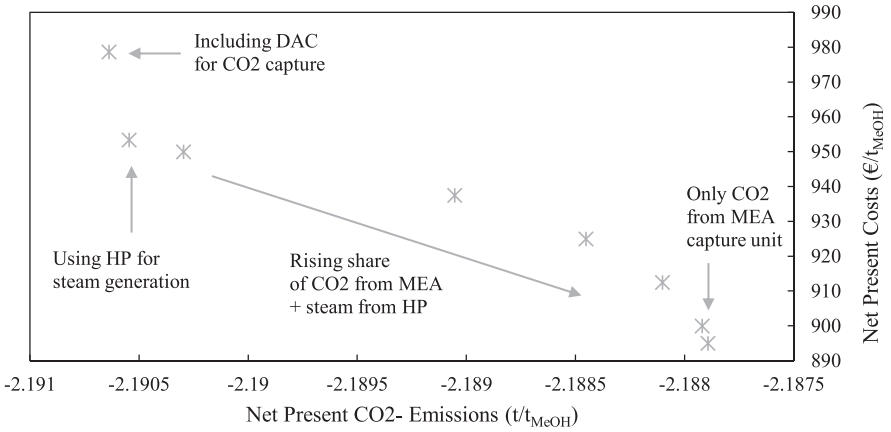

Fig. 8. Pareto-front of Power-to-Methanol optimization.

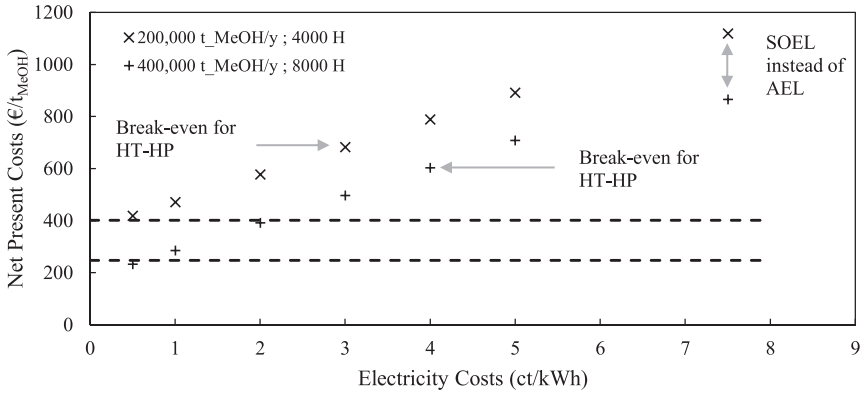

Fig. 9. Sensitivity analysis of net present costs of methanol based on electricity prices and plant capacity (dotted lines represent conventional methanol prices).

ture. The largest share of CO_2 is provided by oxyfuel combustion in a cement factory. Taking a detailed look into the utility-based emissions and heat integration explains this phenomenon. While electricity from wind energy has rather low emission values of 15 kg/MWh, external heat from natural gas shows emissions of around 250 kg/MWh. The CO_2 capture in oxyfuel combustion only requires external electricity, while the cement factory itself produces all the required heat. Hence, the cement factory itself has no environmental benefit, while the synthetic methanol obtains all negative emissions. This concept is the same for the flue gas capture at the refinery. However, the absorption-based CO_2 capture requires additional heat, which is not automatically provided by the refinery itself. Therefore, external steam raises the overall *GWP* emissions. Another difference to the cost-optimal design is, that offgas is converted into steam, which is sold to the market to gain avoided burden credits, rather than utilizing it inside the plant itself.

4.3. Bi-criteria optimization

The difference in plant layout depends on the objective function which indicates trade-off points in terms of costs and global warming potential. To gain a better understanding of these trade-offs a bi-criteria optimization is performed using the equidistant ε – constraint method with inequality constraints (Chircop and Zammit-Mangion, 2013). Using this approach, the GWP-value is optimized while the TAC-value is constrained for 10 equidistant points. The resulting pareto-front is depicted in Fig. 8. It only shows 8 instead of 10 points because some results were equal due to the inequality constraint, while the economic optimization bound was left out due to distortions on the axis. While an emission-optimized design with unconstrainted costs uses DAC as well as MEA only up to the where process internal heat is available, this changes if methanol costs are constrained to 953 €/t_{MeOH}. The share of CO_2 captured by MEA absorption is increased with required lower prices. Simultaneously steam supply by high temperature heat pump is increased to avoid purchase of emission-expensive external steam from natural gas. While the utilization of MEA capture increases, first the usage of DAC decreases. At costs of 900 €/t_{MeOH} also Oxyfuel CO_2 capture is shut down, using only MEA CO_2 capture with steam from heat recovery or high temperature heat pump (HT-HP). Overall it can be observed that NPE only change insignificantly along the pareto-front, with a maximum total difference of 2.75 $kg_{CO2\text{-}eq.}/t_{MeOH}$. On the other hand, high CO_2 savings of 250 $kg_{CO2\text{-}eq}/t_{MeOH}$ compared to the economic optimization can be achieved by providing low pressure steam from high temperature heat pumps with only a small cost penalty of about 3 €/t_{MeOH}, leading to CO_2 abatement costs of 205 €/$t_{CO2\text{-}eq.}$

4.4. Sensitivity analysis

The cost breakdown for synthetic methanol production indicates a strong dependency on the electricity price. To investigate this relation in more detail, a sensitivity analysis is performed, changing the costs of electricity from 7.5 ct/ kWh to 0.5 ct/ kWh. The results are presented in Fig. 9. They indicate that for higher electricity prices of 7.5 ct/kWh, the alkaline electrolysis is replaced by a solid oxide electrolysis indicating a break-even of higher investment costs, low steam costs and high electricity costs. A cost break-even for low pressure steam from a high temperature heat pump is reached at 3 and 4 ct/kWh for low production capacity of 200,000 t/y and full load hours of 4000 h/y as well as high pro-

duction capacities of 400,000 t/y and 8000 full load hours per year, respectively. It is apparent, that with dropping electricity price the overall net production costs of green methanol are decreasing too. At around 1 ct/ kWh, green methanol becomes cost competitive to conventional methanol for production capacities of 200,000 t/y and full load hours (H) of 4000 h/y. Increasing production capacities to 400,000 t/y and full load hours to 8000 h/y, the overall costs decrease about 20 – 40 % depending on the electricity price. This results in minimal costs of 708 €/t_{MeOH} at electricity costs of 5 ct/kWh and cost competitive NPC of 391 €/t_{MeOH} at electricity prices of ca. 2 ct/kWh for large production capacities. This result is in line with Wassermann et al. (2020) and indicates that future production of synthetic methanol with high availability of renewable energies can be cost-competitive to conventional natural gas-based methanol, if economies of scale are considered.

5. Conclusions

A generic model formulation for superstructure optimization was presented. This model is based on mass and energy balances in combination with cost calculation, emission factors and binary decision variables for process design optimization. The optimization model is integrated in OUTDOOR (***O**pen s**U**perstruc**T**ure mo**D**eling and **O**ptimizati**O**n f**R**amework*), a tool which automates data input, pre-processing, as well as results output. Both, the model formulation and OUTDOOR are written in open-source Python code, utilizing the Python-based open-source optimization modeling language (PYOMO) and are uploaded to GitHub. Thereby, providing an intuitive way to access superstructure optimization as well as possibilities to join in the further development of OUTDOOR and the optimization model.

The developed model was applied to a bi-criteria Power-to-Methanol (PtM) optimization case study. Economic and environmental optimal process design of methanol synthesis from different CO_2 capture technologies as well as hydrogen production systems and offgas treatment possibilities were investigated. The results indicate methanol production costs of 892 €/t_{MeOH} and CO_2 emissions of -1.936 $t_{CO\text{-}eq.}/t_{MeOH}$ for cost optimal PtM plants and costs of 979 €/t_{MeOH} with higher CO_2 abatement of -2.191 $t_{CO2\text{-}eq.}/t_{MeOH}$. The high dependency on electricity prices indicate that synthetic methanol could be cost-competitive in the future if renewable electricity becomes cheaper, while production capacities increase exploiting economies of scale.

Declaration of Competing Interest

The authors declare that they have no known competing financial interests or personal relationships that could have appeared to influence the work reported in this paper.

CRediT authorship contribution statement

Philipp Kenkel: Conceptualization, Methodology, Software, Validation, Writing - original draft, Visualization, Data curation, Investigation. **Timo Wassermann:** Conceptualization, Writing - review & editing, Supervision, Project administration, Funding acquisition, Data curation, Validation. **Celina Rose:** Software, Writing - review & editing. **Edwin Zondervan:** Conceptualization, Writing - review & editing, Supervision.

Acknowledgements

Funding of this research by the German Federal Ministry of Economic Affairs and Energy within the KEROSyN100 project (funding code 03EIV051A) is gratefully acknowledged.

References

Albrecht, F.G., König, D.H., Baucks, N., Dietrich, R., 2017. A standardized methodology for the techno-economic evaluation of alternative fuels – a case study. Fuel 194, 511–526. doi:10.1016/j.fuel.2016.12.003.

Baliban, R.C., Elia, J.A., Weekman, V., Floudas, C.A., 2012. Process synthesis of hybrid coal, biomass, and natural gas to liquids via Fischer-Tropsch synthesis, ZSM-5 catalytic conversion, methanol synthesis, methanol-to-gasoline, and methanol-to-olefins/distillate technologies. Comput. Chem. Eng. doi:10.1016/j.compchemeng.2012.06.032.

Bertran, M.O., Frauzem, R., Sanchez-Arcilla, A.S., Zhang, L., Woodley, J.M., Gani, R., 2017. A generic methodology for processing route synthesis and design based on superstructure optimization. Comput. Chem. Eng. 106, 892–910. doi:10.1016/j.compchemeng.2017.01.030.

Bisschop, J., 2016. AIMMS Modeling Guide - Integer Programming Tricks.

Chen, Q., Kale, S., Bates, J., Valentin, R., Bernal, D.E., M., B., Grossmann, I.E., 2019. Pyosyn: A Collaborative Ecosystem for Process Design Advancement. AIChE Annu. Meet. AIChE..

Chircop, K., Zammit-Mangion, D., 2013. On-constraint based methods for the generation of Pareto frontiers. J. Mech. Eng. Autom. 3, 279–289.

Ciric, A.R., Floudas, C.A., 1991. Heat exchanger network synthesis without decomposition. Comput. Chem. Eng. 15, 385–396. doi:10.1016/0098-1354(91)87017-4.

Czyzyk, J., Mesnier, M., Moré, J., 1998. The NEOS server. IEEE Comput. Sci. Eng. 5, 68–75.

Dolan, E.D., 2001. NEOS Server 4.0 Administrative Guide. ariXiv prepprint cs/0107034.

Fasihi, M., Efimova, O., Breyer, C., 2019. Techno-economic assessment of CO2 direct air capture plants. J. Clean. Prod. doi:10.1016/j.jclepro.2019.03.086.

Friedler, F., Aviso, K., Bertok, B., Foo, D.C., R.R., T., 2019. Prospects and challenges for chemical process synthesis with P-graph. Curr. Opin. Chem. Eng. 26, 58–64.

Galanopoulos, C., Kenkel, P., Zondervan, E., 2019. Superstructure optimization of an integrated algae biorefinery. Comput. Chem. Eng. 130, 106530.

Gardarsdottir, S.O., De Lena, E., Romano, M., Roussanaly, S., Voldsund, M., Pérez-Calvo, J.F., Berstad, D., Fu, C., Anantharaman, R., Sutter, D., Gazzani, M., Mazzotti, M., Cinti, G., 2019. Comparison of technologies for CO 2 capture from cement production—Part 2: Cost analysis. Energies 12. doi:10.3390/en12030542.

Gong, J., You, F., 2015. Value-added chemicals from microalgae: Greener, more economical, or both? ACS Sustain. Chem. Eng. 3, 82–96. doi:10.1021/sc500683w.

Horne, R., Grant, T., Verghese, K., 2009. Life cycle assessment: principles, practice, and prospects.

Kenkel, P., Wassermann, T., Zondervan, E., 2020. Design of a Sustainable Power-to-methanol Process: a Superstructure Approach Integrated with Heat Exchanger Network Optimization. Comput. Aided Chem. Eng. 48, 1411–1416.

Kong, L., Sen, S.M., Henao, C.A., Dumesic, J.A., Maravelias, C.T., 2016. A superstructure-based framework for simultaneous process synthesis, heat integration, and utility plant design. Comput. Chem. Eng. 91, 68–84. doi:10.1016/j.compchemeng.2016.02.013.

Kong, Q., Shah, N., 2017. Development of an Optimization-Based Framework for Simultaneous Process Synthesis and Heat Integration. Ind. Eng. Chem. Res. 56, 5000–5013. doi:10.1021/acs.iecr.7b00549.

Kravanja, Z., Grossmann, I.E., 1990. Prosyn-an MINLP process synthesizer. Comput. Chem. Eng. 14, 1363–1378. doi:10.1016/0098-1354(90)80018-7.

Mencarelli, L., Chen, Q., Pagot, A., Grossmann, I., 2020. A review on superstructure optimization approaches in process system engineering. Comput. Chem. Eng., 106808.

Methanex [WWW Document], 2019. "Durchschnittlicher Pr. für Methanol auf dem Eur. Markt den Jahren von 2012 bis 2019 (in Euro je Tonne)." Chart. 19. November, 2019. Stat. Zugegriffen am 26. Novemb. 2019 https//de.statista.com/statistik/daten/studie/.

Morrison, R., 2008. SOS2 constraints in GLPK [WWW Document]. http://winglpk.sourceforge.net/media/glpk-sos2_02.pdf.

Proost, J., 2019. State-of-the art CAPEX data for water electrolysers, and their impact on renewable hydrogen price settings. Int. J. Hydrogen Energy 44, 4406–4413. doi:10.1016/j.ijhydene.2018.07.164.

Quaglia, A., Gargalo, C.L., Chairakwongsa, S., Sin, G., Gani, R., 2015. Systematic network synthesis and design : Problem formulation, superstructure generation, data management and solution. Comput. Chem. Eng. 72, 68–86. doi:10.1016/j.compchemeng.2014.03.007.

Smolinka, T., Wiebe, N., Sterchele, P., Palzer, A., Lehner, F., Jansen, M., Kiemel, S., Miehe, R., Wahren, S., Zimmermann, F., 2018. Industrialisierung der Wasserelektrolyse in Deutschland: Chancen und Herausforderungen für nachhaltigen Wasserstoff für Verkehr. Strom und Wärme, Natl. Organ. Wasserstoff-und Brennstoffzellentechnologie (NOW GmbH).

Statista [WWW Document], 2020. Gaspreise* für Gewerbe- und Ind. Deutschl. den Jahren 2009 bis 2019 (in Euro-Cent pro Kilowattstunde). Zugegriffen am 23.November 2020 https//de.statista.com/statistik/daten/studie/168528/umfrage/gaspreise-fuer-gewerbe–und-industriek.

Tian, Y., Sam Mannan, M., Kravanja, Z., Pistikopoulos, E.N., 2018. Towards the synthesis of modular process intensification systems with safety and operability considerations - application to heat exchanger network. Computer Aided Chemical Engineering. Elsevier B.V., pp. 705–710. doi:10.1016/B978-0-444-64235-6.50125-X.

Tula, A.K., Babi, D.K., Bottlaender, J., Eden, M.R., Gani, R., 2017. A computer-aided software-tool for sustainable process synthesis-intensification. Comput. Chem. Eng. 105, 74–95.

Voldsund, M., Gardarsdottir, S.O., De Lena, E., Pérez-Calvo, J.F., Jamali, A., Berstad, D., Fu, C., Romano, M., Roussanaly, S., Anantharaman, R., Hoppe, H., Sutter, D., Mazzotti, M., Gazzani, M., Cinti, G., Jordal, K., 2019. Comparison of technologies for CO 2 capture from cement production—Part 1: Technical evaluation. Energies 12. doi:10.3390/en12030559.

Wang, L., Chen, M., Küngas, R., Lin, T.E., Diethelm, S., Maréchal, F., Van herle, J., 2019. Power-to-fuels via solid-oxide electrolyzer: Operating window and techno-economics. Renew. Sustain. Energy Rev. 110, 174–187. doi:10.1016/j.rser.2019.04.071.

Wassermann, T., Schnuelle, C., Kenkel, P., Zondervan, E., 2020. Power-to-Methanol at Refineries as a Precursor to Green Jet Fuel Production: a Simulation and Assessment Study, in: Computer Aided Chemical Engineering. Elsevier B.V. 1453–1458. doi:10.1016/B978-0-12-823377-1.50243-3.

Wernet, G., Bauer, C., Steubing, B., Reinhard, J., Moreno-ruiz, E., Weidema, B., 2016. The ecoinvent database version 3 (part I): overview and methodology. Int. J. Life Cycle Assess. 3, 1218–1230. doi:10.1007/s11367-016-1087-8.

Yee, T.F., Grossmann, I.E., 1990. Simultaneous optimization models for heat integration-II. Heat exchanger network synthesis. Comput. Chem. Eng. 14, 1165–1184. doi:10.1016/0098-1354(90)85010-8.

Yee, T.F., Grossmann, I.E., Kravanja, Z., 1990. Simultaneous optimization models for heat integration-I. Area and energy targeting and modeling of multi-stream exchangers. Comput. Chem. Eng. 14, 1151–1164. doi:10.1016/0098-1354(90)85009-Y.

Yeomans, H., Grossmann, I.E., 1999. A systematic modeling framework of superstructure optimization in process synthesis. Comput. Chem. Eng. 23, 709–731. doi:10.1016/S0098-1354(99)00003-4.

Zondervan, E., Nawaz, M., de Haan, A.B., Woodley, J.M., Gani, R., 2011. Optimal design of a multi-product biorefinery system. Comput. Chem. Eng. 35, 1752–1766. doi:10.1016/j.compchemeng.2011.01.042.